PHYSICAL REVIEW A **81**, 050101(R) (2010)

Anharmonicity effects in the bosonic U(2)-SO(3) excited-state quantum phase transition

F. Pérez-Bernal* and O. Álvarez-Bajo

Departamento de Física Aplicada, Facultad de Ciencias Experimentales, Universidad de Huelva, Huelva E-21071, Spain

(Received 7 February 2010; revised manuscript received 18 February 2010; published 14 May 2010)

We study the effect of the inclusion of the U(2) Lie algebra second-order Casimir operator in a model Hamiltonian of the vibron model two-dimensional limit. We extend previously published results, showing that the inclusion of the additional term does not alter the ground-state quantum phase transition between the symmetric and deformed limits of the model. Nevertheless, the inclusion of this operator implies deep changes on the excitation spectrum and on the ensuing excited-state quantum phase transitions.

DOI: 10.1103/PhysRevA.81.050101 PACS number(s): 03.65.Fd, 05.70.Jk, 03.65.Sq, 64.60.−i

Quantum phase transitions (QPTs) as zero-temperature phase transitions driven by the variation of one or more Hamiltonian parameters have drawn significant interest from researchers in fields of physics from condensed matter to nuclear and molecular physics.

Recently, the study of such transitions in algebraic models that associate U($n+1$) as the dynamical algebra for n-dimensional systems has been particularly active. Such models have been successfully applied to different physical problems, in particular to the study of nuclear [1,2] and molecular structures [2,3]. The key feature of the algebraic approach is the study of complex systems from a simple and computationally inexpensive perspective. In particular, algebraic models allow the study of precursors of phase transitions in finite systems.

It is worth emphasizing the pioneer works on shape phase transitions on nuclei [4] that anticipated the detailed construction of the phase diagram of the interacting boson model using either catastrophe theory [4,5], the Landau theory of phase transitions [6,7], or excited levels repulsion and crossing [8]. This field has become a focus of renewed attention after the publication of works on analytical approximations for the spectra of nuclei at or close to the critical point of a shape phase transition [9,10] and the discovery of experimental evidence that matches theoretical predictions [11,12]. Two recent reviews on this subject are [13,14].

These works focus on the so-called ground-state QPTs, also abbreviated as *ground-state transitions* [15]. These transitions take place between different equilibrium shapes of the system and can be compared to structural phase transitions in solid-state physics. Due to the finite system's size, the discontinuities associated with phase transitions are smoothed, though precursors of the phase transition are usually present.

More recently, in the field of algebraic models and QPTs, considerable attention has focused on the so-called excited-state QPTs (ESQPTs). Unlike ground-state QPTs, an ESQPT can take place not only upon variation of a Hamiltonian (control) parameter but also for increasing energy values. ESQPTs occur in excited states [16]. The experimental study of systems undergoing such transitions is hindered by the need for access to highly excited states. This fact has precluded finding a clear example of an ESQPT in nuclear structure. Nevertheless, due to outstanding developments in laser spectroscopy, it is now possible to access highly excited vibrational states. This makes molecular spectroscopy a clear candidate to supply evidence of ESQPT in physical systems.

A particular example of ESQPT that has recently received attention is monodromy in molecular-bending degrees of freedom. Signatures of monodromy are sudden changes of wave-function properties and state density once the excitation energy reaches a critical value. These effects, in the classical limit, can be explained as a pinched-torus singularity that in quantum mechanics implies the lack of a unique set of quantum numbers for the full spectrum of an integrable system [17]. Experimental signatures of monodromy in the vibrational bending spectrum of several molecules have been recently reported [18,19].

In this article, we present results for the two-dimensional limit of the vibron model [3], based on a U(3) dynamical algebra, that can be applied to the modeling of molecular-bending dynamics. Following the algebraic formalism, the molecular-bending Hamiltonian can be constructed from the generators of a two-level bosonic model described by a U(3) Lie algebra [20]. This algebra is generated by the possible bilinear products of a creation and annihilation operator of a singlet boson $(\sigma^\dagger,\sigma)$ and two Cartesian bosons $(\tau_i^\dagger,\tau_i; i=x,y)$, or their circular equivalents $(\tau_i^\dagger,\tau_i; i=+,-)$ [20,21].

The most general, rotational, and parity-invariant one- and two-body Hamiltonian for a two-dimensional system in this approach is characterized by four parameters. The model embodies two possible dynamical symmetries conserving l, the two-dimensional angular momentum. On one hand is the U(3) ⊃ U(2) ⊃ SO(2) dynamical symmetry, associated with rigidly linear molecules. On the other hand is the U(3) ⊃ SO(3) ⊃ SO(2) dynamical symmetry, associated with rigidly bent molecules. A detailed analysis of the ground-state transition that takes place between those two dynamical symmetries is presented in Ref. [21] using the model Hamiltonian

$$\hat{\mathcal{H}} = \varepsilon\left[(1-\xi)\hat{n} + \frac{\xi}{N-1}\hat{P}\right], \tag{1}$$

where the operator $\hat{n} = \tau_+^\dagger\tau_+ + \tau_-^\dagger\tau_-$ is the first-order Casimir operator of U(2), while $\hat{P} = N(N+1) - \hat{W}^2$, and $\hat{W}^2$ is the second-order Casimir operator of SO(3). The parameter N is equal to the total number of bosons in the system, ε is an energy scale, and ξ is the control parameter.

*francisco.perez@dfaie.uhu.es

The classical limit of Hamiltonian (1) can be obtained using the coherent (or intrinsic) state approach, presented in Ref. [15] and applied to the vibron model in Refs. [22,23]. From the obtained energy functional, it has been shown that the system undergoes a second-order QPT, in the mean field limit, for the critical value $\xi_c = 0.2$ of the control parameter [21]. For finite N values, the discontinuity in the second-order derivative of the system's ground-state energy is smoothed out, but precursors of the phase transition are evident, even for low N values, as shown with a numerical study in Ref. [21]. The effects provoked when crossing the critical value of the control parameter on the vibrational energy spectrum [24] and intensities [25] are well known.

The bosonic U(3) model is a simple yet nontrivial model that gives access not only to a well-known ground-state transition, but also to an ESQPT, that appears for control parameter values $\xi > \xi_c$. In fact, the bosonic U(3) algebra is the simplest bosonic two-level model with nontrivial angular momentum. The characteristics of ESQPTs in two-level boson models, including the two-dimensional vibron model using Hamiltonian (1), have been recently presented in Ref. [16]. The ESQPT evidence in the model can be connected to the appearance of monodromy [21,26]. The study of monodromy and ESQPT in the field of molecular spectroscopy is particularly relevant because, to our knowledge, this is the only field where highly excited states can be experimentally accessed and there are available data around the critical point of an ESQPT. This has made monodromy a successful tool for analyzing such spectra [18,19,27].

In the present article, we extend the model Hamiltonian (1) with the inclusion of the second-order Casimir operator of U(2),

$$\hat{\mathcal{H}} = \varepsilon \left[(1-\xi)\hat{n} + \frac{\alpha}{N-1}\hat{n}(\hat{n}+1) + \frac{\xi}{N-1}\hat{P} \right]. \quad (2)$$

The inclusion of this term is necessary to fit bending vibrational data [24,25,28,29]. As in the previous case, the ξ parameter acts as a control parameter, and the linear (symmetrical) geometrical configuration is recovered for $\xi = 0$, while a bent limit is achieved for $\xi = 1$. If the α parameter is different from zero, the $\xi = 0$ limit is transformed from a truncated two-dimensional harmonic oscillator to an anharmonic oscillator. We also stress that for $\xi = 1$ the SO(3) dynamical symmetry is not recovered unless $\alpha = 0$.

The classical or mean field limit of Hamiltonian (2) is obtained using the quoted coherent state approach, giving as a result the energy functional

$$\mathcal{E}_{\xi,\alpha}(r) = \varepsilon \frac{\xi + \{1 - 3\xi + [2\alpha/(N-1)]\}r^2 + \{1 + \alpha + [2\alpha/(N-1)]\}r^4}{(1+r^2)^2}, \quad (3)$$

where r is the dimensionless two-dimensional radial coordinate [21]. In the large N limit, the energy functional becomes

$$\mathcal{E}_{\xi,\alpha}(r) = \varepsilon \frac{\xi + (1-3\xi)r^2 + (1+\alpha)r^4}{(1+r^2)^2}. \quad (4)$$

It can be shown that the system's ground state undergoes a symmetry-breaking second-order phase transition from a linear to a bent geometrical configuration. The variation of the control parameter α does not modify the ground-state-transition characteristics. The main point of the present article is the significant effects on the system's ESQPT that appear for negative α values. The minimization of the energy functional (4) provides the equilibrium values

$$r_e = 0, \quad \sqrt{\frac{5\xi - 1}{3\xi + 2\alpha + 1}}. \quad (5)$$

For $\xi \leqslant \xi_c = 0.2$, the minimum is at the origin, while for values of ξ greater than ξ_c, the minimum at the origin is replaced by a maximum, and a new minimum appears. From Eq. (5), negative values of α have as a lower bound $-(1+3\xi)/2$. When evaluated for $r = r_e$ and $\varepsilon = 1$, the energy functional is

$$\mathcal{E}_{\xi,\alpha}(r_e) = \begin{cases} \xi & 0 \leqslant \xi \leqslant \xi_c \\ \frac{-9\xi^2 + 10\xi + 4\alpha\xi - 1}{16\xi + 4\alpha} & \xi_c < \xi \leqslant 1 \end{cases}. \quad (6)$$

By evaluating the derivatives of $\mathcal{E}_{\xi,\alpha}(r_e)$ with respect to ξ, one finds that the second derivative is discontinuous at $\xi = \xi_c$:

$$\frac{\partial^2 \mathcal{E}_{\xi,\alpha}(r_e)}{\partial \xi^2} = \begin{cases} 0 & 0 \leqslant \xi \leqslant \xi_c \\ -\frac{(4+5\alpha)^2}{2(4\xi+\alpha)^3} & \xi_c < \xi \leqslant 1 \end{cases}. \quad (7)$$

The derivative with respect to α is zero at all orders for $\xi = \xi_c$. Thus, the ground-state QPT of Hamiltonian (2) is of second order, r_e can be considered the classical order parameter, and it is akin to the Hamiltonian (1) ground-state transition [21].

In contrast with the ground-state QPT, there are significant differences between the ESQPT in the original and the new model Hamiltonian. For $\xi > \xi_c$, we define $f_0(\xi,\alpha)$ as the difference between the values of the energy functional (4) evaluated at the local maximum in the origin ($r = 0$) and at the $r = r_e$ minimum (5). This value is the monodromy critical energy, and it defines a separatrix between excited states with different character. In the large N limit, the separatrix is

$$f_0(\xi,\alpha) = \frac{(5\xi - 1)^2}{4(4\xi + \alpha)}, \quad (8)$$

which for $\alpha = 0$ coincides with the separatrix calculated in Ref. [21]. In Fig. 1, we depict the excitation-energy spectra of eigenstates of Hamiltonian (2) with angular momentum $l = 0$ as a function of the control parameter ξ for $N = 80$, $\varepsilon = 1$, and $\alpha = 0$ and -0.4. In both cases, in addition to the correlation

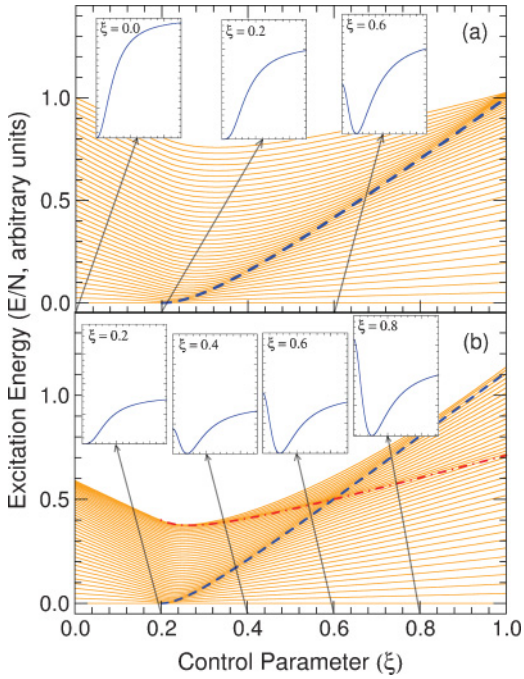

FIG. 1. (Color online) Excitation-energy spectrum for $l = 0$ eigenstates of Hamiltonian (2) as a function of the control parameter ξ, with $N = 80$, $\varepsilon = 1$, and anharmonicity parameter values $\alpha = 0, -0.4$ (upper and lower panels, respectively). The insets display the energy functional (4) for selected values of the control parameter ξ. The abscissa and ordinate scaling is common to all the insets, and the energy minimum is fixed to zero in all cases.

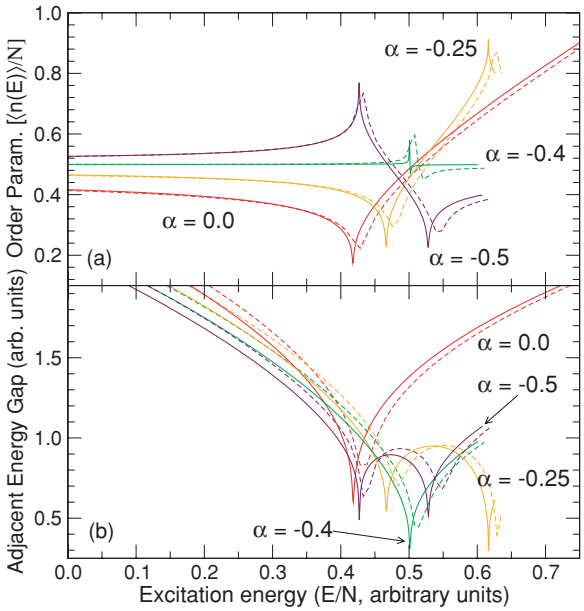

FIG. 2. (Color online) (a) Expectation value of $\hat{n}$ as a function of the excitation energy. Both quantities are divided by N for normalization purposes. (b) Excitation-energy dependence of the adjacent levels energy gap. In both cases, calculations are performed for $l = 0$ eigenvectors of the Hamiltonian (2) with $\varepsilon = 1$, $\xi = 0.6$, $N = 80$ (dashed lines), and $N = 800$ (solid lines).

energy diagram, we have included insets depicting the energy functional (4) for selected values of the control parameter ξ.

The $\alpha = 0$ case (no anharmonic contribution) is depicted in the upper panel of Fig. 1. As is well established, the energy functional minimum remains in the origin for ξ values between zero [first inset, Fig. 1(a)] and the critical value of the control parameter $\xi_c = 0.2$ [second inset, Fig. 1(a)]. The energy functional becomes more level as ξ increases. If $\xi > \xi_c$, the minimum in the origin is replaced by a maximum, and a minimum appears for $r_e \neq 0$ [e.g., third inset in Fig. 1(a)]. A thick blue dashed line marks the separatrix (8), signaling the high density of states, which is connected with the monodromy critical point. Therefore, the separatrix divides the excited states into two sets: under the curve are those with bent character and above the curve are those with linear character. This is a well-known result [16,21], and the inclusion of positive α values does not qualitatively alter this diagram. However, a major change occurs when considering negative α values. The separatrix (8), marked in the lower panel of Fig. 1 with a thick blue dashed line, still indicates a line of transition between eigenstates of different characters, but a second line with a high density of states appears. This second line is associated with a new separatrix, $f_1(\xi,\alpha)$, defined as the difference between the asymptotic value of the energy functional, $\lim_{r\to\infty} \mathcal{E}_{\xi,\alpha}(r)$, and the value at the $r = r_e$ minimum,

$$f_1(\xi,\alpha) = \frac{(3\xi + 2\alpha + 1)^2}{4(4\xi + \alpha)}. \tag{9}$$

This new separatrix is plotted in the lower panel of Fig. 1 with a thick red dot-dashed line. The insets in this panel show the energy functional (4) for selected values of ξ. The more relevant feature is that for $\xi > \xi_c = 0.2$, the value of the energy functional in the origin can be less (e.g., $\xi = 0.4$ inset), equal (e.g., $\xi = 0.6$ inset), or more (e.g., $\xi = 0.8$ inset) than the limit of the energy functional value for large r values.

Following Refs. [16,21], we proceed to define quantities acting as order parameters for the ESQPT. It is important to emphasize that ESQPT order parameters differ from traditional order parameters in that they are not zero on one side of the transition. However, they still mark the excitation energy where the transition occurs. In the upper panel of Fig. 2, we depict the expectation value of the $U(2)$ number operator, $\hat{n}$, as a function of the energy for $l = 0$ eigenstates of Hamiltonian (2) with $N = 80,800$, $\xi = 0.6$, and different α values. In the lower panel, for the same set of eigenstates, we plot the energy gap between adjacent levels (known as a Birge-Sponer plot in molecular spectroscopy). In both cases, the $\alpha = 0$ case coincides with the results published in Ref. [16]. However, for negative α values, both quantities show novel features in the high-energy region. In the $\langle\hat{n}\rangle/N$ case, a maximum appears at the energy where the second zone of high density of states is located in Fig. 1(b). The energy functional depicted in the $\xi = 0.4$ inset is an example of this case, where $\mathcal{E}_{\xi,\alpha}(0) < \lim_{r\to\infty} \mathcal{E}_{\xi,\alpha}(r)$. The new maximum moves toward lower energies for increasing $|\alpha|$ values, until a critical value $\alpha_c = \xi - 1$, given by the condition $f_0(\xi,\alpha_c) = f_1(\xi,\alpha_c)$. The $\xi = 0.6$ inset shows the energy functional in this case, with $\mathcal{E}_{\xi,\alpha_c}(0) = \lim_{r\to\infty} \mathcal{E}_{\xi,\alpha_c}(r)$. In this latter case, the expectation value of $\hat{n}$ becomes constant in the full excitation-energy range, apart from a sudden oscillation that takes place at the

energy where the two separatrices cross. If the value of α keeps decreasing, the minimum at low energies is replaced by a maximum and vice versa. The $\xi = 0.8$ inset in Fig. 1(b) presents an energy functional example in this case, where $\mathcal{E}_{\xi,\alpha}(0) > \lim_{r\to\infty} \mathcal{E}_{\xi,\alpha}(r)$.

In the energy-gap plot (lower panel of Fig. 2), the situation is quite similar. There is a first minimum corresponding to the critical energy associated with the monodromy, joined by a second minimum at high energies for $\alpha < 0$, which moves toward lower energies for increasing $|\alpha|$ values. Both minima coincide if $\alpha = \alpha_c$. For smaller α values, we find again two minima in the plot.

We have performed the calculations for Fig. 2 with $N = 80$ (dashed lines) and $N = 800$ (solid lines), showing that precursors of the ESQPT already exist for $N = 80$. They become much sharper for $N = 800$, as expected.

As in [16], the angular momentum degeneracy varies when going across an ESQPT line. This is shown in Fig. 3, where the excitation-energy spectra of $l = 0$ and 1 eigenstates as a function of ξ are depicted for $N = 80$, $\varepsilon = 1$, and $\alpha = -0.4$. This figure clearly shows how once a separatrix line is crossed, degeneracy changes. The two separatrices divide the states in four different regions.

We have thus shown that the inclusion of the U(2) second-order Casimir operator in the model Hamiltonian of the two-dimensional limit of the vibron model does not alter the ground-state QPT properties, but there is a qualitative change in the ESQPT structure. As discussed, the experimental access to states at or across the ESQPT has been possible in the field of molecular spectroscopy. A detailed account of the present calculations as well as fits to different molecular spectra using the U(3) limit of the vibron model will be presented in another paper [29]. Experimental detection of the features shown in the present article will be of great interest. As they take place at high excitation energies, they may be affected by energy redistribution between vibrational degrees of freedom, an effect that should be taken into account.

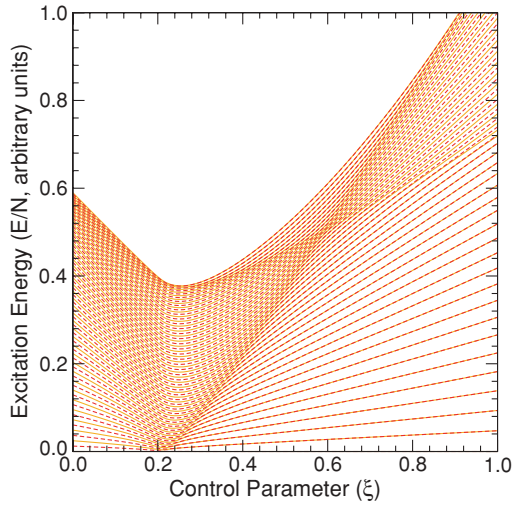

FIG. 3. (Color online) Excitation-energy spectrum of $l = 0$ (solid orange lines) and $l = 1$ (dashed red lines) eigenstates of Hamiltonian (2) as a function of ξ. The rest of parameters are fixed to $N = 80$, $\varepsilon = 1$, and $\alpha = -0.4$.

This work was supported in part by the Spanish Junta de Andalucía under projects P07-FQM-02962 and P07-FQM-03014. We gratefully acknowledge useful discussion with F. Iachello, J. M. Arias, M. Carvajal, and J. E. García-Ramos.

[1] F. Iachello and A. Arima, *The Interacting Boson Model* (Cambridge University Press, Cambridge, 1987).
[2] A. Frank and P. van Isacker, *Algebraic Methods in Molecular and Nuclear Structure Physics* (John Wiley and Sons, New York, 1994).
[3] F. Iachello and R. D. Levine, *Algebraic Theory of Molecules* (Oxford University Press, Oxford, 1995).
[4] D. H. Feng, R. Gilmore, and S. R. Deans, Phys. Rev. C **23**, 1254 (1981).
[5] E. López-Moreno and O. Castaños, Phys. Rev. C **54**, 2374 (1996).
[6] F. Iachello, N. V. Zamfir, and R. F. Casten, Phys. Rev. Lett. **81**, 1191 (1998).
[7] J. Jolie *et al.*, Phys. Rev. Lett. **89**, 182502 (2002).
[8] J. M. Arias, J. Dukelsky, and J. E. García-Ramos, Phys. Rev. Lett. **91**, 162502 (2003).
[9] F. Iachello, Phys. Rev. Lett. **85**, 3580 (2000).
[10] F. Iachello, Phys. Rev. Lett. **87**, 052502 (2001).
[11] R. F. Casten and N. V. Zamfir, Phys. Rev. Lett. **85**, 3584 (2000).
[12] R. F. Casten and N. V. Zamfir, Phys. Rev. Lett. **87**, 052503 (2001).
[13] R. F. Casten, Prog. Part. Nucl. Phys. **62**, 183 (2009).
[14] P. Cejnar and J. Jolie, Prog. Part. Nucl. Phys. **62**, 210 (2009).
[15] R. Gilmore, J. Math. Phys. **20**, 891 (1979).
[16] M. A. Caprio, P. Cejnar, and F. Iachello, Ann. Phys. **323**, 1106 (2008).
[17] M. S. Child, J. Phys. A **31**, 657 (1998).
[18] B. P. Winnewisser *et al.*, Phys. Rev. Lett. **95**, 243002 (2005).
[19] N. F. Zobov *et al.*, Chem. Phys. Lett. **414**, 193 (2006).
[20] F. Iachello and S. Oss, J. Chem. Phys. **104**, 6956 (1996).
[21] F. Pérez-Bernal and F. Iachello, Phys. Rev. A **77**, 032115 (2008).
[22] O. S. van Roosmalen, Ph.D. thesis, University of Groningen, 1982.
[23] O. S. van Roosmalen, R. D. Levine, and A. E. L. Dieperink, Chem. Phys. Lett. **101**, 512 (1983).
[24] F. Iachello, F. Pérez-Bernal, and P. H. Vaccaro, Chem. Phys. Lett. **375**, 309 (2003).
[25] F. Pérez-Bernal, L. F. Santos, P. H. Vaccaro, and F. Iachello, Chem. Phys. Lett. **414**, 398 (2005).
[26] S. Heinze, P. Cejnar, J. Jolie, and M. Macek, Phys. Rev. C **73**, 014306 (2006).
[27] M. Winnewisser *et al.*, J. Mol. Struct. **798**, 1 (2006).
[28] H. Ishikawa *et al.*, Chem. Phys. Lett. **365**, 57 (2002).
[29] O. Álvarez-Bajo *et al.* (unpublished).